Pharmacophore modeling and in silico screening for new KDR kinase inhibitors

Hui Yu,[a] Zhanli Wang,[b] Liangren Zhang,[c] Jufeng Zhang[a] and Qian Huang[a,*]

[a]*Central Experimental Laboratory, The First People's Hospital, Shanghai Jiaotong University, Shanghai 200080, China*
[b]*Technology Center, NeoTrident Technology Ltd, Beijing 100080, China*
[c]*School of Pharmaceutical Science, Peking University, Beijing 100083, China*

Abstract—In order to elucidate the essential structural features for KDR kinase inhibitors, three-dimensional pharmacophore hypotheses were built on the basis of a set of known KDR kinase inhibitors selected from the literature with CATALYST program. Several methods tools used in validation of pharmacophore hypothsis were presented, and the first hypothesis (Hypo1) was considered to be the best pharmacophore hypothesis. The model (Hypo1) was then employed as 3D search query to screen the Traditional Chinese Medicine Database (TCMD) for other potential lead compounds. One hit illustrated high binding affinity with KDR kinase measured by the surface plasmon resonance biosensor. Docking studies may help elucidate the mechanisms of KDR kinase receptor–ligand interactions.
© 2007 Elsevier Ltd. All rights reserved.

Vascular endothelial growth factor (VEGF) plays pivotal roles in many angiogenic processes both in normal and pathological conditions.[1,2] VEGF binds tyrosine kinase receptors Flk-1 (also known as VEGF receptor 2, KDR as human counterpart)[3] with high affinity and regulates angiogenesis during the development of solid tumors. The inhibition of VEGF-Flk-1/KDR signal transduction might be promising for the treatment of highly vascularized tumors.

A considerable number of activity data for KDR kinase inhibitors that belong to diverse chemical classes are currently available. Several compounds such as SU5416,[4] PTK787,[5] and CP-547632[6] have been reported to inhibit KDR kinase at low micromolar concentration. A pharmacophore model based on the binding of ATP to the hinge region of the kinase domain of VEGFR has been developed by Nagarajan Pattabiraman and co-workers.[7] Recently, a series of compounds representing a new class revealed very high activities and strong selectivity for the inhibition of the KDR kinase.[8–13] As the number of synthetic inhibitors of KDR kinase increases, it becomes important to elucidate the structure–activity relationships (SAR) of these diverse compounds.[14] We investigated ligand-based pharmacophores for KDR kinase inhibitors to inform the design process for new selective inhibitors and to gain a greater understanding of the structure–KDR kinase inhibitory activity relationships, which combined CATALYST HypoGen approach[15] with a training set selection method.
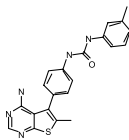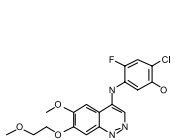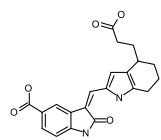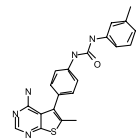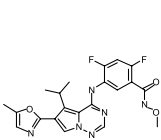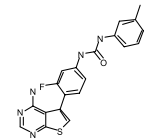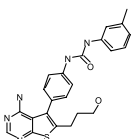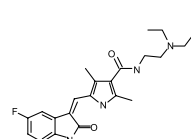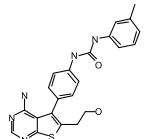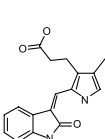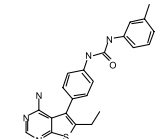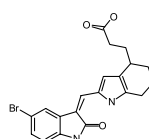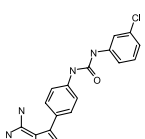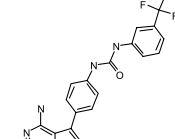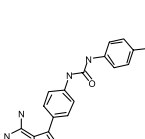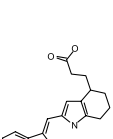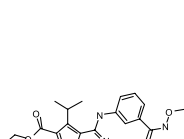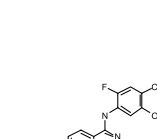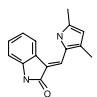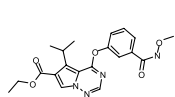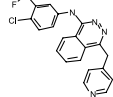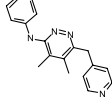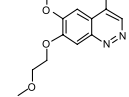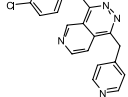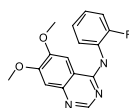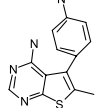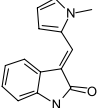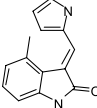
In this study, feature-based three-dimensional model for KDR kinase inhibitors was developed, and the model was then used as a search query for the Traditional Chinese Medicine Database (TCMD) searching in an attempt to find new classes of compounds with affinity for the KDR kinase. Potential lead compound was selected for further in vitro study. Docking studies may help elucidate the mechanisms of KDR kinase receptor–ligand interactions.

Twenty-eight compounds forming the training set were used to generate pharmacophores, and biological activity data of 28 compounds span over 5 orders of magnitude. Binding assays are reported in detail elsewhere.[8–13] Structures of these compounds are listed below in Table 1. The compounds were built using the CATALYST 2D/3D visualizer in CATALYST 4.10

Table 1. Chemical structures and activity data (IC_{50} values, μM) of the 28 training set molecules applied to HypoGen pharmacophore generation

1 , 0.003 μM   2 , 0.004 μM   3 , 0.004 μM   4 , 0.006 μM   5 , 0.008 μM   6 , 0.011 μM

7 , 0.015 μM   8 , 0.018 μM   9 , 0.019 μM   10 , 0.02 μM   11, 0.026 μM   12 , 0.03 μM

13 , 0.035 μM   14 , 0.052 μM   15 , 0.053 μM   16 , 0.09 μM   17 , 0.13 μM   18 , 0.15 μM

19 , 0.2 μM   20 , 0.27 μM   21 , 0.3 μM   22 , 0.87 μM   23 , 1.1 μM   24 , 1.4 μM

25 , 2.7 μM   26 , 4.6 μM   27 , 20 μM   28 , 31 μM

software package and were minimized to the closest local minimum using the CHARMm-like force field implemented in the program.[16] CATALYST generated a representative family of conformational models for each compound using the Poling Algorithm and the 'best conformational analysis' method.[17–19] Diverse conformational models for each compound were generated using an energy range of 20 kcal/mol of the calculated potential energy minimum. Specify 250 as the maximum number of conformers of each molecule to ensure maximum coverage of the conformational space. After preparing lead set of molecules, generating a conformational model for each one, we chose the functions to be used and then set up a background process to generate a hypothesis.

Pharmacophores were computed and the top 10 hypotheses were exported. Results of pharmacophore hypotheses are presented in Table 2. The first hypothesis (Hypo1) is the best pharmacophore hypothesis in this study, characterized by the highest cost difference (75.184), lowest root-mean-square error (0.947), and the best correlation coefficient (0.911). The fixed cost, pharmacophore cost, and null cost are 108.48, 122.026, and 197.21, respectively. Hypo1 is presented in Figure 1.

Table 2. Information of statistical significance and predictive power presented in cost values measured in bits for top 10 hypotheses as a result of automated HypoGen pharmacophore generation process[a]

Hypothesis no.	Total cost	Δcost	RMS deviation	Correlation
1	122.026	75.184	0.94745	0.910977
2	122.715	74.495	0.97764	0.904688
3	123.451	73.759	1.02323	0.894325
4	126.741	70.469	1.12766	0.870113
5	129.698	67.512	1.21125	0.848652
6	130.865	66.345	1.23152	0.843869
7	131.090	66.120	1.25973	0.834611
8	131.216	65.994	1.26864	0.831770
9	131.330	65.880	1.26906	0.831778
10	131.904	65.306	1.22785	0.847449

[a] Null cost of 10 top-scored hypotheses is 197.21. Fixed cost value is 108.48. Configuration cost is 13.174.

Figure 2 shows the Hypo1 aligned with the highest active compound **1** (IC_{50} = 0.003 μM) of the training set.

Besides this cost analysis, another validation method to characterize the quality of Hypo1 is represented by its capacity for correct activity prediction. Table 3 shows
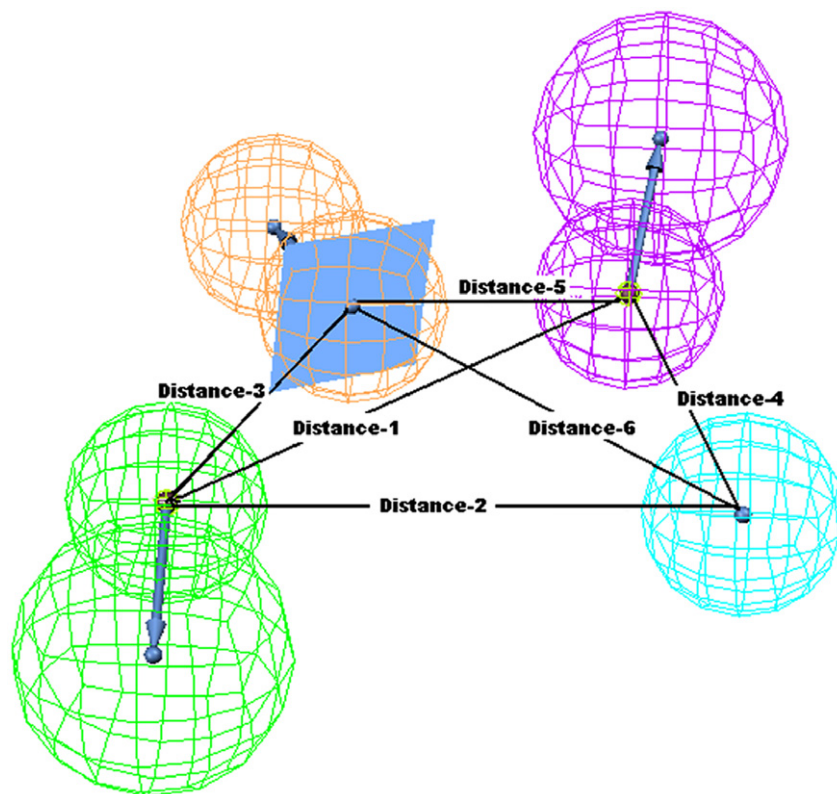
Figure 1. CATALYST HypoGen pharmacophore model illustrating hydrophobic (blue); ring aromatic (orange), hydrogen bond donor (purple), and hydrogen bond acceptor (green). Distance-1, 9.723 Å; Distance-2, 11.997 Å; Distance-3, 3.974 Å; Distance-4, 3.025 Å; Distance-5, 6.370 Å, and Distance-6 9.004 Å.
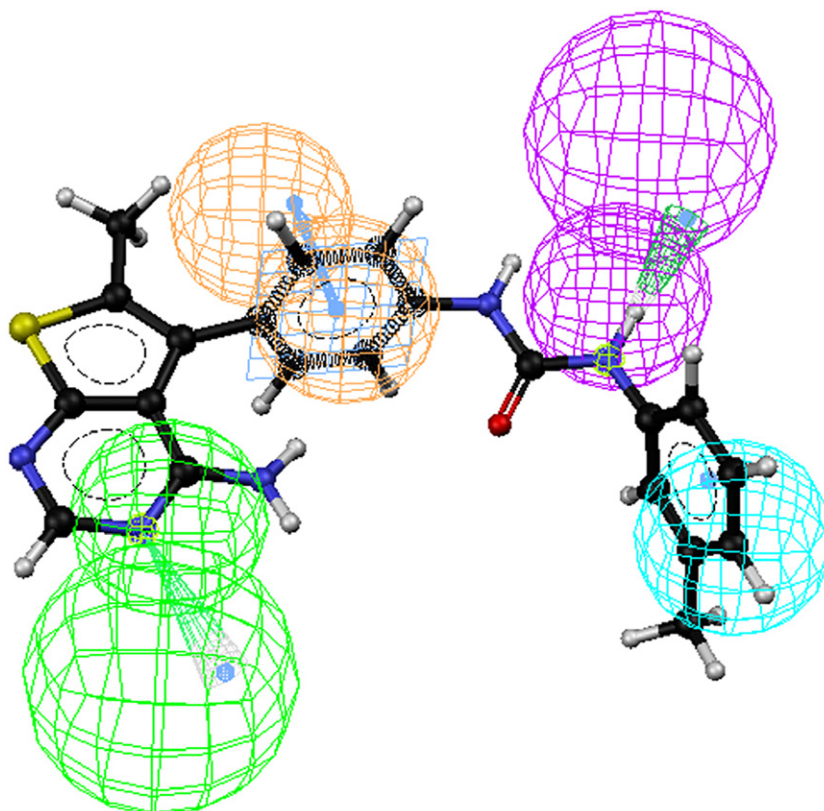
Figure 2. Best HypoGen pharmacophore model Hypo1 aligned to training set compound 1 (IC_{50} = 0.003 μM). Pharmacophore features are color-coded (hydrophobic, blue; ring aromatic, orange; hydrogen bond donor, purple; hydrogen bond acceptor, green).

Table 3. Experimental biological data and estimated IC_{50} of training set molecules based on pharmacophore model Hypo1

Compound	Actual IC_{50} (μM)	Estimated IC_{50} (μM)	Error	Ref.
1	0.003	0.009	+3.0	8
2	0.004	0.0029	−1.4	11
3	0.004	0.001	−3.9	12
4	0.006	0.017	+2.8	8
5	0.008	0.093	+12	9
6	0.011	0.028	+2.5	8
7	0.015	0.029	+2.0	8
8	0.018	0.099	+5.5	8
9	0.019	0.014	−1.4	8
10	0.02	0.028	+1.4	12
11	0.026	0.037	+1.4	8
12	0.03	0.13	+4.4	12
13	0.035	0.024	−1.4	8
14	0.052	0.028	−1.9	8
15	0.053	0.075	+1.4	8
16	0.09	0.062	−1.4	12
17	0.13	0.12	−1.1	9
18	0.15	0.51	+3.4	11
19	0.2	0.13	−1.6	11
20	0.27	0.071	−3.8	9
21	0.30	0.26	−1.2	13
22	0.87	0.43	−2.0	13
23	1.1	0.099	−11	11
24	1.4	0.5	−2.8	11
25	2.7	2.4	−1.1	11
26	4.6	2.8	−1.6	8
27	20	160	−1.3	10
28	31	9.4	−3.3	10

the actual and estimated inhibitory activities of the 28 molecules from the training set based on the pharmacophore model hypothesis, Hypo1. The difference between estimated activity values and experimental activity values is represented as error (ratio between the estimated and experimental activity), with a negative sign if the actual activity is higher than that of the estimated. As we can see from Table 3, most compounds were predicted correctly.

The validity and the predictive character of Hypo1 were further assessed by using the test set molecules. A test set containing 20 molecules of different activity classes was analyzed (Tab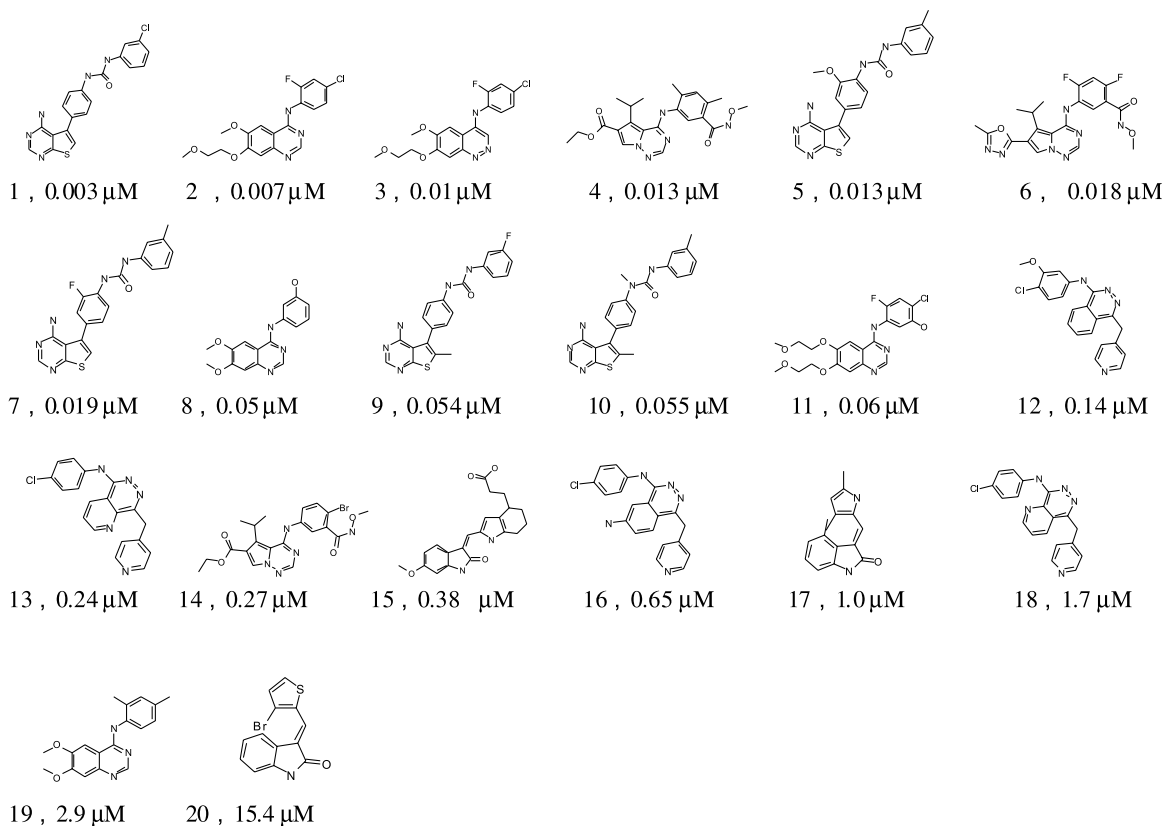le 4). All test set molecules were built and minimized as well as used in conformational analysis like all training set compounds. Hypo1 was regressed against the test set compounds. A score of 81.89% was achieved. In the test set analysis, most of the IC_{50} values were predicted correctly. The results are presented in Table 5.

Finally, cross validation using the CatScramble program available in CATALYST was applied to assess the statistical confidence of Hypo1. The goal of this type of validation is to check whether there is a strong correlation between the structures and activity. CatScramble mixes up activity values of all training set compounds and creates 19 random spreadsheets. In this validation test, we select the 95% confidence level. The results are presented in Figure 3.

Table 4. Chemical structures and activity data (IC_{50} values, μM) of the 20 test set molecules

1 , 0.003 μM   2 , 0.007 μM   3 , 0.01 μM   4 , 0.013 μM   5 , 0.013 μM   6 , 0.018 μM

7 , 0.019 μM   8 , 0.05 μM   9 , 0.054 μM   10 , 0.055 μM   11 , 0.06 μM   12 , 0.14 μM

13 , 0.24 μM   14 , 0.27 μM   15 , 0.38 μM   16 , 0.65 μM   17 , 1.0 μM   18 , 1.7 μM

19 , 2.9 μM   20 , 15.4 μM

Table 5. Experimental biological data and estimated IC_{50} of test set molecules based on pharmacophore model Hypo1

| Compound	Actual IC_{50} (µM)	Estimated IC_{50} (µM)	Error	Ref.
1	0.003	0.015	+5.0	8
2	0.007	0.057	+8.1	11
3	0.01	0.061	+6.1	11
4	0.013	0.018	+1.4	8
5	0.013	0.061	+4.7	9
6	0.018	0.16	+8.9	9
7	0.019	0.01	−1.9	8
8	0.05	0.22	+4.3	11
9	0.054	0.081	+1.5	8
10	0.055	0.11	+2.0	8
11	0.06	0.26	+4.3	11
12	0.14	0.36	+2.6	13
13	0.24	0.41	+1.7	13
14	0.27	0.096	−2.8	9
15	0.38	0.082	−4.6	12
16	0.65	0.41	−1.6	13
17	1.0	1.7	+1.7	10
18	1.7	0.42	−4.1	13
19	2.9	1.2	−2.4	11
20	15.4	15	−1	10

We employed the first hypothesis (Hypo1) as 3D-search query against the Traditional Chinese Medicine Database (TCMD), using the 'fast flexible search' approach implemented within CATALYST. The pharmacophore captured 392 hits from a commercially available database of 10,458 compounds. The molecules identified included a broad range of templates that were structurally diverse from the starting molecule. The hits were subsequently fitted against the Hypo1 and the highest ranking 20 compounds were selected for being further investigated as potential new structures for design of novel KDR kinase inhibitors.

Lipinski 'rule of five' to the problem of recognizing 'drug-like' molecules has been employed. With this tool, it appears possible to identify compounds which have desirable or 'drug-like' properties. Results indicated that one compound (Compound_Number_5688) satisfies the

demands of Lipinski 'rule of five'. This compound was evaluated as KDR kinase inhibitor in vitro, and SPR biosensor technology[20] was used to directly measure the binding interactions of small ligand to KDR kinase using the dual flow cell Biacore 3000 instrument (Biacore AB, Uppsala, Sweden). For kinetic analysis, various concentrations of small ligand were injected for 60s at a flow rate of 20 µl/min to allow for binding with KDR kinase immobilized on the chip surface. The Biacore biosensor determination results for the binding of the ligand with immobilized KDR kinase are shown in Figure 4. For the KDR kinase, hit compound resulted in a significant and dose-dependent increase in SPR response units (RU). The hit compound concentration series were fitted to a steady-state binding model encoded in the Biacore 3000 evaluation software for binding affinity determination. The dissociation constant (K_d value) between the hit compound and KDR kinase was determined as 30 µM.

In addition, Affinity program within InsightII was used for docking of hit compound into the KDR kinase binding site, which was taken from a crystal structure (PDB code: 1YWN),[21] and so we could learn the mechanisms of KDR kinase receptor–ligand interactions. Figure 5
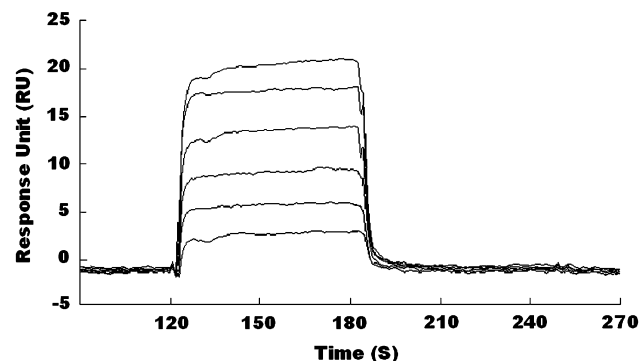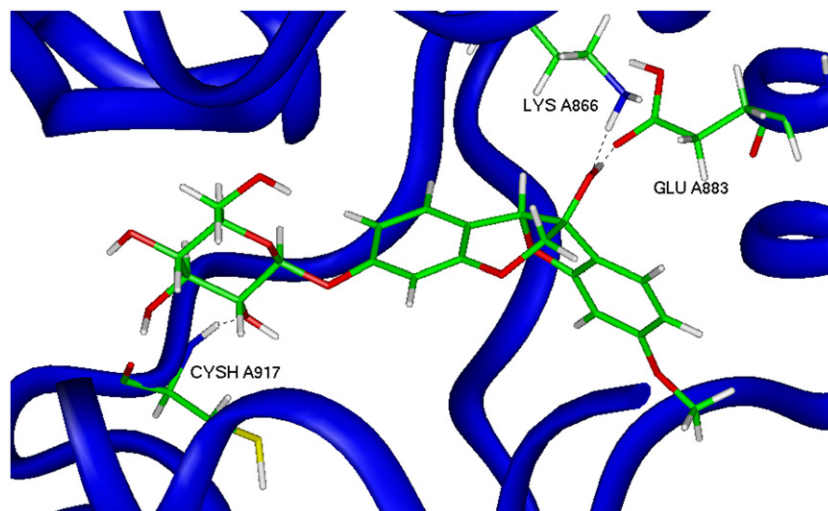

Figure 4. Binding affinity of hit compound to the KDR kinase evaluated by Biacore 3000. Sensorgrams obtained from the injections of hit over the immobilized KDR kinase surface at concentrations of 80, 40, 20, 10, 5, and 2.5 µM (curves from top to bottom).
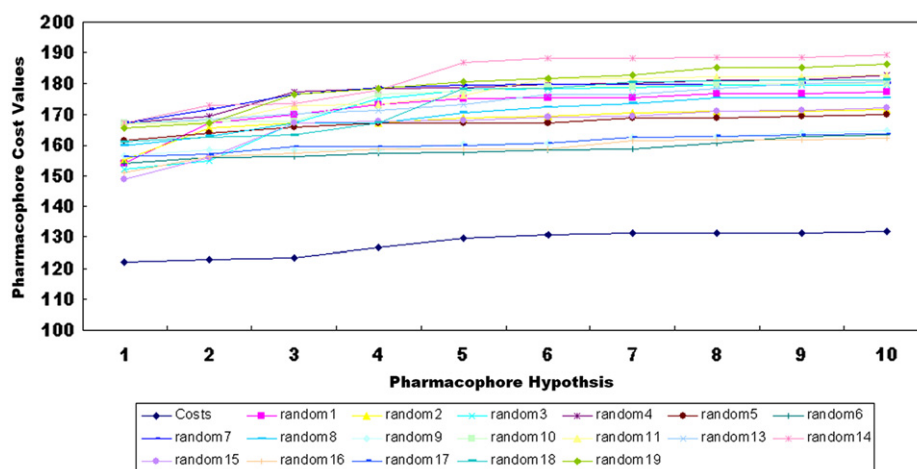
Figure 3. The difference in costs between the HypoGen runs and the scrambled runs. The 95% confidence level was selected.
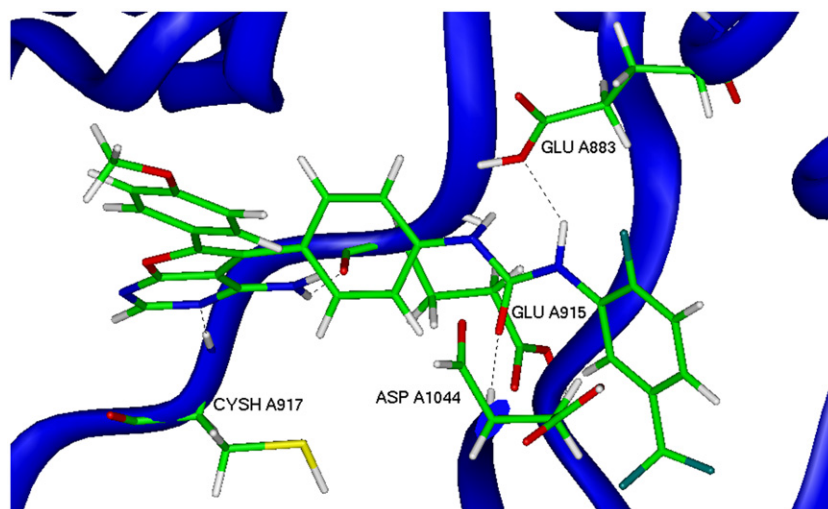
Figure 5. Model of hit compound bound to KDR kinase (PDB code: 1YWN). Hydrogen bonds in black are shown.

shows a possible energy-minimized docking model of KDR kinase-inhibitor. From docking results we know that several hydrogen bonds are formed between hit compound and KDR kinase. Interestingly, one of the hydroxyl oxygens of hit compound and the Cys 917 of KDR kinase form H-bond interaction, one of the hydroxyl groups of hit compound and Lys 866, Glu 883 of KDR kinase also form optimal H-bond interaction. The modeling also suggested that the hydrophobic of hit compound contacted with a hydrophobic region, which is comprised of the side chains of Ile 886, Leu 887, Ile 890, Val 896, and Leu 1017. These interactions lead to a large stabilization of compound in this region. This binding motif is in agreement with other studies.[22] Figure 6 shows the binding mode of KDR kinase with 4-amino-furo[2,3-d] pyrimidine (PDB code: 1YWN).

The alignment of the Hypo1 with hit compound (Fig. 7) was compared with the energy-minimized docking model of KDR kinase-inhibitor. A marked similarity was observed between the hit compound binding features in the energy-minimized docking model and that proposed by the Hypo1. This result confirmed clearly that the specific interaction between KDR kinase and hit compound was consistent with that proposed by the phamacophore.

In summary, pharmacophore model Hypo1 was obtained from the set of KDR kinase inhibitors. Hypo1 consists of one hydrophobic, one hydrogen bond acceptor, one hydrogen bond donor, and one ring aromatic function. This pharmacophore model was able to accurately predict known inhibitors, and the validation results also provide additional confidence in the proposed pharmacophore model. The model was then employed as 3D search query to screen the Traditional Chinese Medicine Database (TCMD). The pharmacophore captured 392 hits, and the highest ranking 20 compounds were selected for being further investigated. Lipinski 'rule of five' to the problem of recognizing 'drug-like' molecules has been employed, one compound satisfies the demands of Lipinski 'rule of five'. This hit compound illustrated high KDR kinase

Figure 6. Model of 4-amino-furo [2,3-d] pyrimidine bound to KDR kinase (PDB code: 1YWN). Hydrogen bonds in black are shown.
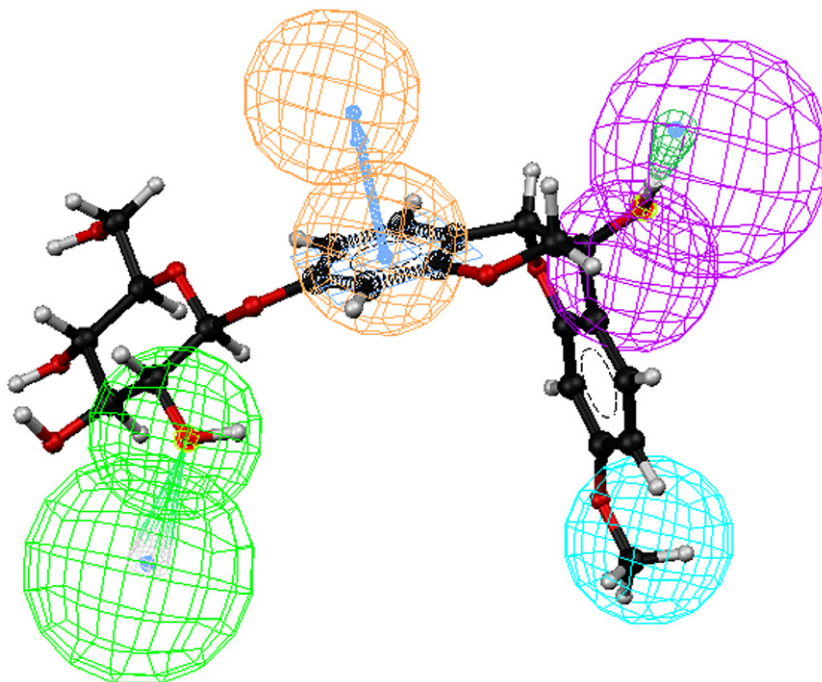
Figure 7. Best HypoGen pharmacophore model Hypo1 aligned to hit compound. Pharmacophore features are color-coded (hydrophobic, blue; ring aromatic, orange; hydrogen bond donor, purple; hydrogen bond acceptor, green).

binding affinity measured by the surface plasmon resonance biosensor. In addition, docking studies were surely help to elucidate the mechanisms of protein–inhibitor interaction.

Supplementary data

Supplementary data associated with this article can be found, in the online version, at doi:10.1016/j.bmcl.2007.01.089.

References and notes

1. Ferrara, N. *Endocr. Rev.* **2004**, *25*, 581.
2. Shibuya, M.; Yamaguchi, S.; Yamane, A.; Ikeda, T.; Tojo, A.; Matsushime, H.; Sato, M. *Oncogene* **1990**, *5*, 519.
3. Millauer, B.; Wizigmann-Voos, S.; Schnurch, H.; Martinez, R.; Moller, N. P.; Risau, W.; Ullrich, A. *Cell* **1993**, *72*, 835.
4. Stopeck, A.; Sheldon, M.; Vahedian, M.; Cropp, G.; Gosalia, R.; Hannah, A. *Clin. Cancer Res.* **2003**, *8*, 2798.
5. Bold, G.; Altmann, K. H.; Frei, J.; Lang, M.; Manley, P. W.; Traxler, P.; Wietfeld, B.; Bruggen, J.; Buchdunger, E.; Cozens, R.; Ferrari, S.; Furet, P.; Hofmann, F.; Martiny-Baron, G.; Mestan, J.; Rosel, J.; Sills, M.; Stover, D.; Acemoglu, F.; Boss, E.; Emmenegger, R.; Lasser, L.; Masso, E.; Roth, R.; Schlachter, C.; Vetterli, W.; Wyss, D.; Wood, J. M. *J. Med. Chem.* **2000**, *43*, 2310.
6. Roberts, W. G.; Jani, J.; Beebe, J.; Emerson, E.; Gant, T.; Goodwin, P.; Higdon, C.; Hillerman, S.; Intrieri, C.; Knauth, E.; Marx, M.; Noe, M.; Rossi, A. M.; Savage, D.; Atherton, J.; Schaeffer, T.; Floyd, E.; Harriman, S. *Proc. Am. Soc. Clin. Oncol.* **2002**, Abstract #473.
7. Sridhar, J.; Akula, N.; Sivanesan, D.; Narasimhan, M.; Rathinavelu, A.; Pattabiraman, N. *Bioorg. Med. Chem. Lett.* **2005**, *15*, 4125.
8. Dai, Y.; Guo, Y.; Frey, R. R.; Ji, Z.; Curtin, M. L.; Ahmed, A. A.; Albert, D. H.; Arnold, L.; Arries, S. S.; Barlozzari, T.; Bauch, J. L.; Bouska, J. J.; Bousquet, P. F.; Cunha, G. A.; Glaser, K. B.; Guo, J.; Li, J.; Marcotte, P. A.; Marsh, K. C.; Moskey, M. D.; Pease, L. J.; Stewart, K. D.; Stoll, V. S.; Tapang, P.; Wishart, N.; Davidsen, S. K.; Michaelides, M. R. *J. Med. Chem.* **2005**, *48*, 6066.
9. Borzilleri, R. M.; Zheng, X.; Qian, L.; Ellis, C.; Cai, Z-W.; Wautlet, B. S.; Mortillo, S.; Jeyaseelan, R.; Kukral, D. W.; Fura, A.; Kamath, A.; Vyas, V.; Tokarski, J. S.; Barrish, J. C.; Hunt, J. T.; Lombardo, L. J.; Fargnoli, J.; Bhide, R. S. *J. Med. Chem.* **2005**, *48*, 3991.
10. Sun, L.; Tran, N.; Tang, F.; App, H.; Hirth, P.; McMahon, G.; Tang, C. *J. Med. Chem.* **1998**, *41*, 2588.
11. Hennequin, L. F.; Thomas, A. P.; Johnstone, C.; Stokes, E. S. E.; Plé, P. A.; Lohmann, J. M.; Ogilvie, D. J.; Dukes, M.; Wedge, S. R.; Curwen, J. O.; Kendrew, J.; Lambert-van der Brempt, C. *J. Med. Chem.* **1999**, *42*, 5369.
12. Sun, L.; Tran, N.; Liang, C.; Hubbard, S.; Tang, F.; Lipson, K.; Schreck, R.; Zhou, Y.; Waltz, K.; McMahon, G.; Tang, C. *J. Med. Chem.* **2000**, *43*, 2655.
13. Bold, G.; Altmann, K. H.; Frei, J.; Lang, M.; Manley, P.; Traxler, P.; Weitfeld, B.; Brueggen, J.; Buchdunger, E.; Cozens, R.; Ferrari, S.; Furet, P.; Hofmann, F.; Martiny-Baron, G.; Mestan, J.; Roesel, J.; Sills, M.; Stover, D.; Acemoglu, F.; Boss, E.; Emmenegger, R.; Laesser, L.; Masso, E.; Roth, R.; Schlachter, C.; Vetterli, W.; Wyss, D.; Wood, J. M. *J. Med. Chem.* **2000**, *43*, 2310.
14. Boyer, S. J. *Curr. Top. Med. Chem.* **2002**, *2*, 973.
15. Nicklaus, M. C.; Neamati, N.; Hong, H.; Mazumder, A.; Sunder, S.; Chen, J.; Milne, G. W.; Pommier, Y. *J. Med. Chem.* **1997**, *40*, 920.

16. Brooks, B. R.; Brucolleri, R. E.; Olafson, B. D.; States, D. J.; Swaminathan, S.; Karplus, M. *J. Comput. Chem.* **1983**, *4*, 187.
17. Smellie, A.; Teig, S. L.; Towbin, P. *J. Comput. Chem.* **1995**, *16*, 171.
18. Smellie, A.; Kahn, S. D.; Teig, S. L. *J. Chem. Inf. Comput. Sci.* **1995**, *35*, 285.
19. Smellie, A.; Kahn, S. D.; Teig, S. L. *J. Chem. Inf. Comput. Sci.* **1995**, *35*, 295.
20. Spiga, O.; Bernini, A.; Scarselli, M.; Ciutti, A.; Bracci, L.; Lozzi, L.; Lelli, B.; Maro, D. D.; Calamandrei, D.; Niccolai, N. *FEBS Lett.* **2002**, *511*, 33.
21. *InsightII*, Version 2005; Accelrys Inc.: San Diego, CA, 2005.
22. Miyazaki, Y.; Matsunaga, S.; Tang, J.; Maeda, Y.; Nakano, M.; Philippe, R. J.; Shibahara, M.; Liu, W.; Sato, H.; Wang, L.; Nolte, R. T. *Bioorg. Med. Chem. Lett.* **2005**, *15*, 2203.